Rock Mech. Rock Engng. (2002) 35 (4), 225–254
DOI 10.1007/s00603-002-0026-0

Rock Mechanics and Rock Engineering
Printed in Austria

Manuel Rocha Medal Recipient

Simulating the Time-dependent Behaviour of Excavations in Hard Rock

By

D. F. Malan

CSIR Mining Technology, Johannesburg, South Africa

Received January 15, 2002; accepted June 3, 2002
Published online September 2, 2002 © Springer-Verlag 2002

This paper summarises some of the work presented by Dr. D. F. Malan during the ISRM Rocha medal ceremony at the 2nd Asian Rock Mechanics Symposium in Beijing, China during September 2001. Dr. Malan was born and educated in South Africa and completed his PhD studies at the University of the Witwatersrand in 1998. He is currently the Programme Manager for the Rock Engineering programme at CSIR Mining Technology in Johannesburg.

Summary

Although hard rock is not usually associated with large creep deformation, data collected from the tunnels and stopes of the deep South African gold mines illustrates significant time-dependent behaviour. Apart from application in mining, a better understanding of the time-dependent behaviour of crystalline rock is required to analyse the long term stability of nuclear waste repositories and to design better support for deep civil engineering tunnels in these rock types. To illustrate the subtle problems associated with using viscoelastic theory to simulate the time-dependent behaviour of hard rock, a viscoelastic convergence solution for the incremental enlargement of a tabular excavation is discussed. Data on the time-dependent deformation of a tunnel developed in hard rock further illustrates the limitations of the theory, as it is unable to simulate the fracture zone around these excavations. To simulate the rheology of the fracture zone, a continuum viscoplastic approach was developed and implemented in a finite difference code. This proved more successful in modelling the time-dependent closure of stopes and squeezing conditions in hard rock tunnels. A continuum approach, however, has limitations in areas where the squeezing behaviour is

dominated by the time-dependent behaviour of prominent discontinuities such as bedding planes. To overcome this problem, a viscoplastic displacement discontinuity technique was developed. This, combined with a tessellation approach, leads to more realistic modelling of the time-dependent behaviour of the fracture zone around excavations.

1. The Need for Research into the Time-dependent Behaviour of Hard Rock

In a previous paper, Malan (1999a) described the need for research into the time-dependent behaviour of the deep tabular excavations in the South African gold mining industry. Although the focus of this earlier paper was mainly on the closure behaviour of deep tabular excavations, the results formed part of a larger study of the time-dependent behaviour of hard rock. As the findings of this study have important implications in areas of rock mechanics outside the mining industry, it is summarised in this paper with emphasis on application in tunneling excavations. Further details on this study of the time-dependent behaviour of hard rock can be found in Malan (1998), Malan (1999b), Napier and Malan (1997) and Malan and Drescher (2000). It should be noted that this current paper deals exclusively with the time-dependent behaviour of hard crystalline rock and the squeezing behaviour of tunnels in soft rocks, such as shale or potash, will not be considered. For more information on the time-dependent behaviour of tunnels in weak rock, the reader is referred to a special issue of the Italian Geotechnical Journal (2000) dealing exclusively with squeezing conditions in tunnels.

Outside of the South African mining industry, an engineering application where the time-dependent behaviour of hard rock recently became more important is the study of long-term stability of chambers used for nuclear waste repositories (Blacic, 1981; Pusch, 1993). Although many of these repositories are located in salt and potash (e.g. Kwon, 2000), some are planned in crystalline rock such as granite (Kwon et al., 2000). An important aspect of the problem is that the excavations must be maintained for many decades to allow retrieval of waste and monitoring of repository performance. According to the design criteria for Yucca mountain repository in the United States, the closure rates in the main access drift and other drifts need to be below 1 mm/year and 3 mm/year, respectively. Although, intuitively, damage to excavations in hard rock from time-dependent deformation seems unlikely, Blacic (1981) showed that time-dependent microcracking and water-induced stress corrosion can lead to significant reductions in strength in the near field region of a repository. The issue of roof stability of these repositories is also important. Although these roofs may remain stable for hundreds of years, depending on the rock type, excavation dimensions and stress conditions, problems may appear soon after development as noted in the hard rock mines in South Africa. Pusch (1993) estimated the rock disintegration of the roof of the Swedish repository at Forsmark where the excavation is intersected by a fracture zone. By generalising the structure to be one of regular layers of blocks and applying a log-time creep law, he estimated that the roof would disintegrate to a depth of 3 m over a period of a thousand years.

Further research on the time-dependent behaviour of hard rock is also necessary to determine the onset of squeezing conditions in deep tunnels developed in

hard rock. An example of the ever-increasing depth of civil engineering tunnels is the Gotthard Base Tunnel being developed in southern central Switzerland where the maximum overburden is approximately 2500 m (Brox and Hagedorn, 1996). It is not clear if the existing empirical rules to predict squeezing are still valid at these great depths for crystalline rock. For tunneling in soft rock, an empirical rule frequently used to identify squeezing conditions is the competency factor c. This is defined as the ratio of the uniaxial compressive strength of the rock to the overburden stress (Muirwood, 1972; Nakano, 1979; Barla, 1995; Aydan et al., 1996) and is calculated as

$$c = \frac{\sigma_c}{\rho g H} \tag{1}$$

where σ_c is the uniaxial compressive strength of intact laboratory specimens, ρ is the density of the rock, g is gravitational acceleration and H is the depth below surface. In general, squeezing conditions are found for $c < 2$. This was confirmed by Aydan et al. (1996) who did an extensive survey of squeezing tunnels in Japan. The depth of tunnels in this study was less than 400 m and the host rock comprised typical soft types like mudstone, tuff, shale and siltstone. It is therefore unclear if this simple rule can be extended to deep tunnels in hard rock.

1.1 Tunnel Deformation at Hartebeestfontein Mine

Experience of the behaviour of access tunnels in the deep South African gold mines showed that rock displacements reminiscent of squeezing in weak rock can occur, even though these tunnels are developed in hard crystalline rock. One example is the large tunnel deformation observed at the Hartebeestfontein Mine near Klerksdorp in South Africa (Malan and Bosman, 1997). The tunnels in question are developed in argillaceous quartzites with a uniaxial compressive strength ranging from 130 MPa to 180 MPa. The combination of relatively weak quartzites and high stress leads to appreciable time-dependent movement of the rock and severe support difficulties. In some cases, extreme tunnel closure rates in the order of 50 cm per month have been reported (Malan and Basson, 1998). Figure 1 illustrates typical conditions in tunnels experiencing significant time-dependent deformation at the mine. This necessitates frequent rehabilitation of these tunnels. If the time-dependent fracture processes could be better understood, optimum strategies could be developed to reduce the cost of continually installing new support.

To illustrate typical rates of closure in the squeezing tunnels at Hartebeestfontein Mine, data from a measuring station in the 78A24 East haulage in the No. 6 shaft area is illustrated below. The tunnel was developed in argillaceous quartzites with an average uniaxial compressive strength of 177 MPa. The quartzites contain well-defined bedding planes.

It would be of interest to measure tunnel closure on the surface of the excavation, but due to the poor rock conditions, closure pegs, which are not anchored deep in the rock, are lost very soon after installation. Therefore, the measuring station consisted of 2.2 m rods grouted in the hangingwall and sidewalls and a

Fig. 1. Adverse haulage conditions at Hartebeestfontein Gold Mine in South Africa caused by slow time-dependent deformation processes in the rock. Note that this is not rockburst damage (courtesy W. D. Ortlepp)

0.4 m rod grouted in the footwall (Fig. 2). The closure measurements were taken between the ends of these rods which protruded from the rock. The position of the measuring station in relation to the surrounding stoping operations is illustrated in Fig. 3.

Sidewall measurements over a period of 180 days are illustrated in Fig. 4. A total closure of 65 mm was measured during this period. For the first 75 days of measurement, there was no mining in this area as the ledging in Fig. 3 only started in September 1996. For this initial period, when the stresses acting on the tunnel were constant, an average closure rate of 0.24 mm/day was measured between the two sidewalls. Note that the magnitude of deformation recorded is less than the surface deformation of the excavation because the measuring rods were anchored deeply in the rock. It is clear that the magnitude of closure measured at this site is unacceptably high for a service excavation that needs to remain stable for many years. Note that the rapid increase in closure rate in September 1996 was not only due to the nearby mining, but also damage caused by a seismic event (magnitude 1.5), which was located approximately 200 m from the measurement station.

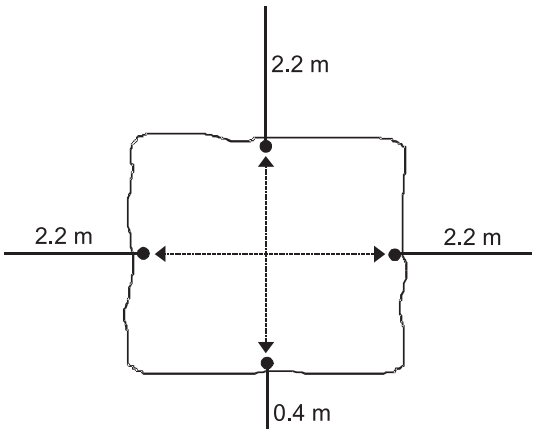

Fig. 2. Closure station consisting of rods grouted deeply in the rock. The deformation illustrated in Fig. 4 was taken between the two rods in the sidewalls

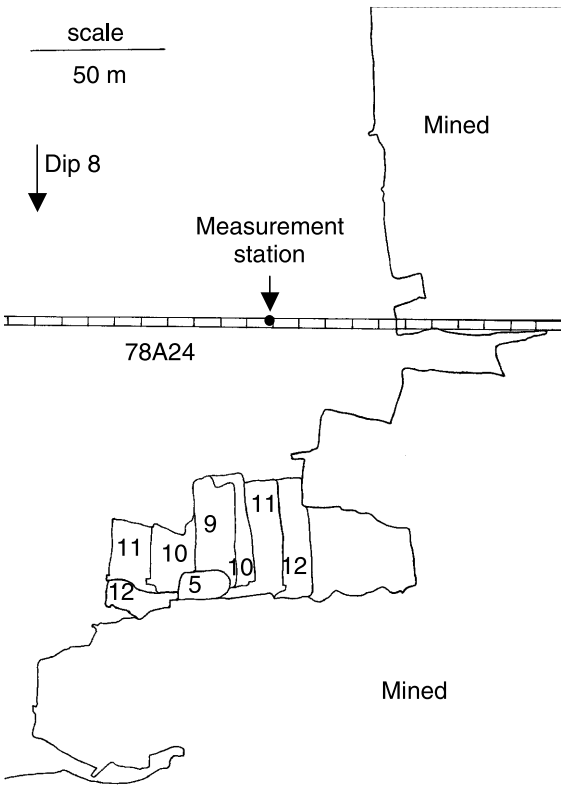

Fig. 3. Plan view of the stoping operations surrounding the measurement station in the haulage. The haulage is approximately 45 m below the reef. The numbers indicate the month in which the particular section was mined in 1996

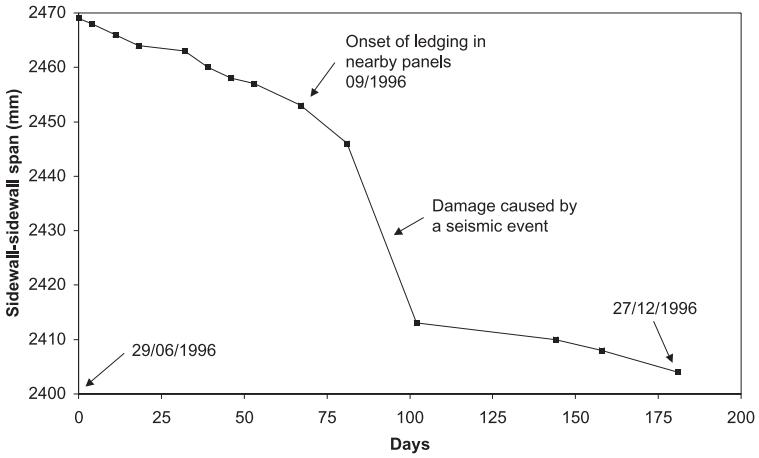

Fig. 4. Sidewall deformation measured in the haulage

This paper is divided in three sections, investigating the implications of using viscoelastic models, continuum elasto-viscoplastic models and a discontinuum viscoplastic model to simulate the time-dependent behaviour of hard rock.

2. Some Notes on the Use of Viscoelastic Theory

The theory of viscoelasticity provides a theoretical basis for analysing time-dependent rock movement and for extrapolation beyond the range of an experimental data set. In linear viscoelastic theory, complex strain-time behaviour can be described by various combinations of two principal states of deformation namely elastic behaviour and viscous behaviour. As no attempt is made to review viscoelastic theory in this text, the reader is referred to Flügge (1975) for a good introduction to the subject. The historical use of different viscoelastic models to simulate the creep of rocks is given in Lama and Vutukuri (1978).

There has always been some doubt about the usefulness of this theory in representing rock behaviour, as explained by Robertson (1964), owing to the functional dependence of the viscosity values on stress, temperature and chemical environments. Some argue that this does not detract from its usefulness as a concept in creep analysis as long as its limitations are clearly understood. Similarly the parameters of linear elasticity theory, when applied to rock, are not constant over a wide range of strain rates and temperatures, but it is nevertheless an important approximation frequently used in rock mechanics. In regards to viscoelasticity, even recent publications can be found were it has been used to simulate time-dependent behaviour of rock (Pan and Dong, 1991a). In this current study however, it was discovered that there are some subtle problems associated with the use of viscoelasticity theory to simulate time-dependent closure of tabular excavations in hard rock. Although the example below is not directly relevant to tunnel design and support, it is included to highlight some of the problems associated with vis-

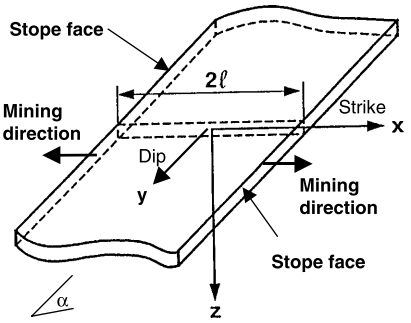

Fig. 5. A single parallel-sided tabular excavation. The analytical viscoelastic convergence solution was derived for the two-dimensional section in the figure. The origin of the co-ordinate system is at the centre of the stope

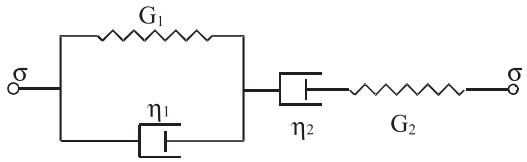

Fig. 6. Representation of the Burgers viscoelastic model with the viscosity coefficients η_1 and η_2 and shear moduli G_1 and G_2

coelastic theory. These problems arise because of the special geometry of the tabular excavations and are not readily apparent when applying the theory to circular tunnels. This is a symptom of the fundamental problem of linear viscoelasticity in relation to rock mechanics, namely the inability to simulate failure.

2.1 Viscoelastic Convergence Solution for Tabular Excavations

Some experimental data of the time-dependent convergence of deep tabular excavations is given in Malan (1999a). As a preliminary attempt to simulate the time-dependent deformations measured in these excavations, a viscoelastic approach was investigated.

As no analytical model for the closure of tabular openings in viscoelastic media was available, a two-dimensional closure solution for a parallel-sided tabular excavation (Fig. 5) in a viscoelastic medium was derived by the author. The solution was obtained by subjecting a known elastic solution to the viscoelastic correspondence principle (Appendix I). An important feature of this analytical solution is that it accounts for the incremental enlargement of these excavations. When assuming that the rock behaves as an elastic material in dilatation and as a Burgers viscoelastic material (Fig. 6) in distortion, the solution for an excavation developed in n increments with both faces blasted simultaneously can be derived as given in Eq. (2) and (3). The various coefficients in these two equations are given in Eq. (4) to (13).

$$S_z = \left\{ \sum_{i=1}^{n-1} [S_z(\ell_i, t-\tau_i)] - [S_z(\ell_i, t-\tau_{i+1})] \right\} + S_z[\ell_n, t-\tau_n] \quad \text{for } \tau_n < t \le \tau_{n+1} \tag{2}$$

where

$$S_z(\ell_i, t-\tau_i) = -4W_z\sqrt{\ell_i^2 - x^2}\left(1 + \frac{dx}{2}\right) \times g_1[1 + c_5 t + c_6 e^{-f(t-\tau_i)} + \{c_7 \sinh b(t-\tau_i) + c_8 \cosh b(t-\tau_i)\} e^{-h(t-\tau_i)/2}], \tag{3}$$

and

$$W_z = \frac{-\rho g H}{2}[(1+k) + (1-k)\cos 2\alpha] \tag{4}$$

$$d = \frac{\sin\alpha \cos\beta}{H} \tag{5}$$

$$b = \sqrt{\frac{(6Kp_1 + q_1)^2 - 24K(6Kp_2 + q_2)}{4(6Kp_2 + q_2)^2}} \tag{6}$$

$$g_1 = \frac{2Kp_1q_1 + q_1^2 - 2Kq_2}{4Kq_1^2} \tag{7}$$

$$c_5 = \frac{2Kq_1}{2Kp_1q_1 + q_1^2 - 2Kq_2} \tag{8}$$

$$c_6 = \frac{2K(p_2q_1^2 - p_1q_1q_2 + q_2^2)}{q_2(2Kp_1q_1 + q_1^2 - 2Kq_2)} \tag{9}$$

$$c_7 = \frac{q_1^2(-12Kp_2q_1 + 6Kp_1q_2 - q_1q_2)}{2b(6Kp_2 + q_2)^2(2Kp_1q_1 + q_1^2 - 2Kq_2)} \tag{10}$$

$$c_8 = \frac{q_1^2 q_2}{(6Kp_2 + q_2)(-2Kp_1q_1 - q_1^2 + 2Kq_2)} \tag{11}$$

$$f = \frac{q_1}{q_2} \quad h = \frac{6Kp_1 + q_1}{6Kp_2 + q_2} \tag{12}$$

$$p_1 = \frac{\eta_1 G_2 + \eta_2 G_1 + \eta_2 G_2}{2G_1G_2} \quad p_2 = \frac{\eta_1\eta_2}{4G_1G_2} \quad q_1 = \eta_2 \quad q_2 = \frac{\eta_1\eta_2}{2G_1}, \tag{13}$$

where S_z is the stope closure, $2\ell_i$ is the span of the stope after mining increment i, ρ is the density of the rock, x is the position in the stope, g is the gravitational acceleration, H is the depth below surface, k is the ratio of horizontal to vertical stress, α is the dip of the reef, β is the angle between the x-axis and the dip, v is Poisson's ratio, E is Young's modulus, n is the number of increments, t is time and

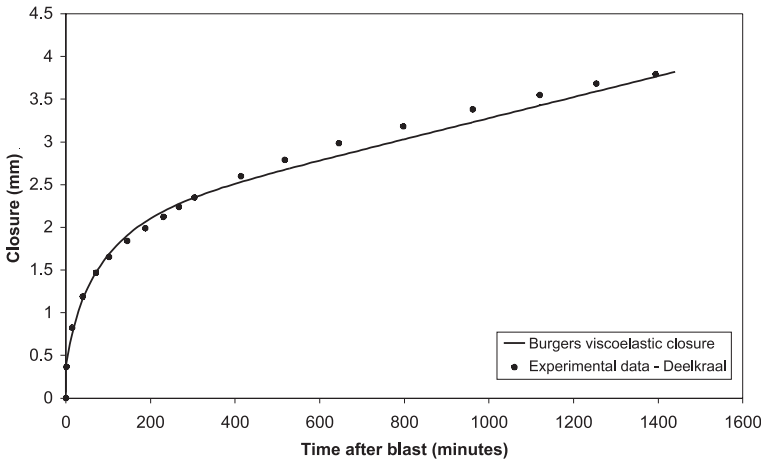

Fig. 7. The Burgers viscoelastic closure solution fitted to experimental closure measured at Deelkraal Mine

τ_i is the time when increment i is mined. The Burgers viscosity coefficients η_1 and η_2 and shear moduli G_1 and G_2 are defined in Fig. 6. It should also be noted that this solution is only valid for stopes where a two-dimensional approximation is possible and where no contact between footwall and hangingwall occurs in the centre of the stope.

Using this approach, a good fit with experimental data could be obtained as shown in Fig. 7 (see Malan, 1998). Although this appears encouraging, problems were noted when attempting to calibrate the model at various distances from the mining face. These problems arise as the model predicts that the rate of steady-state convergence increases towards the center of the stope. This can be shown by taking the time derivative of Eq. (3) (assuming the excavation was made in a single cut, $i = 1$, at time $\tau_1 = 0$). For time $t \to \infty$, the derivative is given by (see Malan, 1998)

$$\left.\frac{dS_z}{dt}\right|_{t\to\infty} = \frac{-2W_z\sqrt{\ell^2 - x^2}\left(1 + \dfrac{dx}{2}\right)}{\eta_2}. \tag{14}$$

As $t \to \infty$, the convergence rate in the secondary phase is therefore only a function of geometric parameters, stress magnitude and the viscoelastic parameter η_2. This is intuitively expected from Fig. 6. Also if $\eta_2 = \infty$ (thereby reducing the Burgers model to the 3-parameter solid, Eq. (4) predicts correctly that at $t \to \infty$, the convergence rate becomes zero. The steady-state convergence rate (Eq. 3) was plotted as a function of the position x in Fig. 8. The highest rate of convergence is in the centre of the stope, which reduces to a value of zero at the stope face. This can be compared with some underground data collected in a South African mining stope, illustrating the opposite trend where the rate of steady-state closure decreases with increasing distance from the stope face. This difference in behaviour is caused

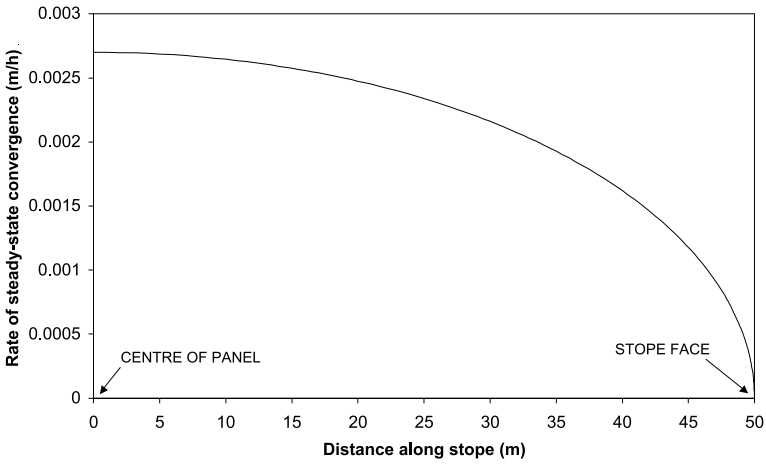

Fig. 8. The rate of steady-state convergence along a panel of 100 m span at $t \rightarrow \infty$. Values used in this simulation are $\eta_2 = 2 \times 10^{12}$ Pa.h, $H = 2000$ m, $\alpha = 0°$, $k = 0.5$, g = 9.81 m/s^2 and $\rho = 2700$ kg/m^3

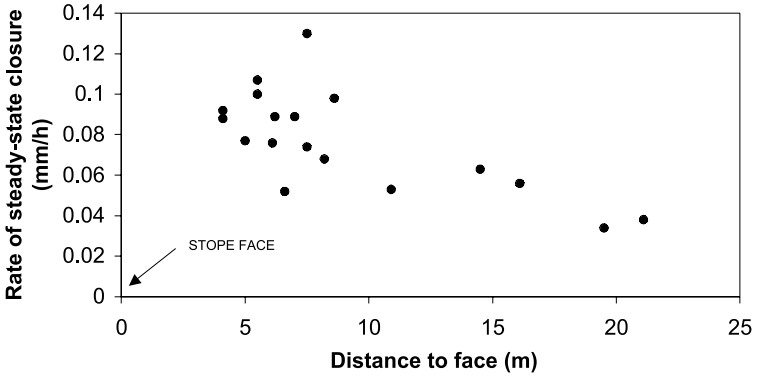

Fig. 9. Closure data from a deep tabular mining stope in South Africa. Note that the rate of steady-state closure decreases as the distance to face increases. This is contrary to what is shown by the viscoelastic model in Fig. 8. (Note that the stope face is to the left in Fig. 9 and to the right in Fig. 8.)

by the inability of the viscoelastic model to simulate the fracture processes surrounding the deep mining excavations.

2.2 Implications when Simulating the Time-dependent Behaviour of Tunnels Using Viscoelastic Theory

In many instances where significant time-dependent tunnel deformation is observed, the temptation exists to measure the rate of deformation between pegs installed on the tunnel surface and then, due to its simplicity, use viscoelastic theory to simulate the data and extrapolate into the future. Good fits with the data can usually be obtained, similarly to what is illustrated for the tabular excavation

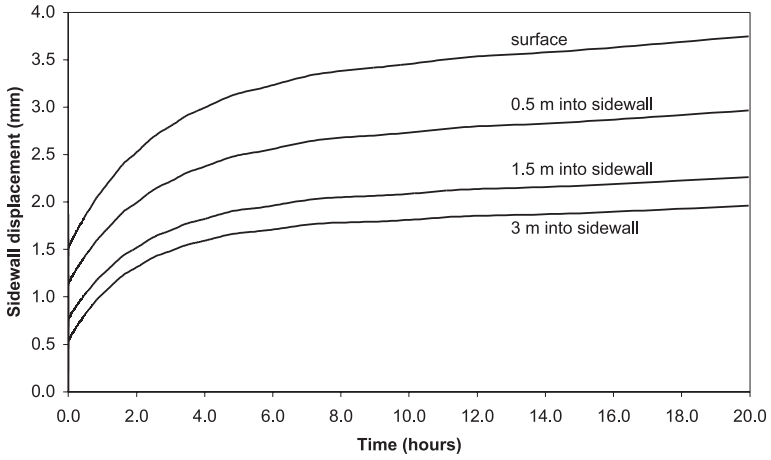

Fig. 10. Numerical solution of the deformation of a tunnel sidewall. The rock is assumed to behave as a Burgers viscoelastic material in distortion. The parameters used were (see Fig. 3): Bulk modulus = 30 GPa, $G_1 = G_2 = 30$ GPa, $\eta_1 = 80$ GPa/h and $\eta_2 = 2000$ GPa/h. The horizontal and vertical stresses were assumed to be 60 MPa

given above in Fig. 7. When there is significant fracturing around the excavation, however, viscoelastic theory cannot be used to estimate the relative movement between the skin of the excavation and some distance inside the rock mass. This was illustrated by simulating a circular tunnel of 3 m diameter in material that is assumed to behave according to the Burgers model in Fig. 6. These simulations were conducted using the creep version of the FLAC code (Itasca, 1993). A Burgers constitutive model, available as a FISH (the built-in programming language in FLAC) routine, was used. Figure 10 illustrates the absolute displacements measured in the tunnel sidewall along a horizontal line. Notice that the amount of displacement gradually decreases with increasing distance into the sidewall.

To compare these results with underground data of excavations in hard rock, Figure 11 shows the deformation of a pump chamber at Hartebeestfontein Mine (Malan, 1998). The chamber was developed in argillaceous quartzites with an average strength of 142 MPa. The dimension of the chamber was 18.5 m $\times$ 6 m $\times$ 3.5 m. The data in Fig. 11 was measured using rod extensometers anchored at different depths in the sidewall. The deformation measured is therefore the relative displacement between the skin of the excavation and a certain depth into the rock mass. Note that there are significant differences in deformation between the anchor points at 2 m and 3 m and also 5 m and 6 m. This is probably caused by fractures or discontinuities opening at these particular depths.

Unfortunately continuum viscoelastic theory is not able to simulate this complex behaviour as seen in Fig. 10 where the deformation gradually decreases with increasing distance into the rock. Although a calibrated viscoelastic model might give a good fit to deformation measured on the skin of the tunnel in hard rock, it cannot be used to design rock bolt support where the relative displacement between the skin of the tunnel and a point at a certain depth in the rock needs to be determined.

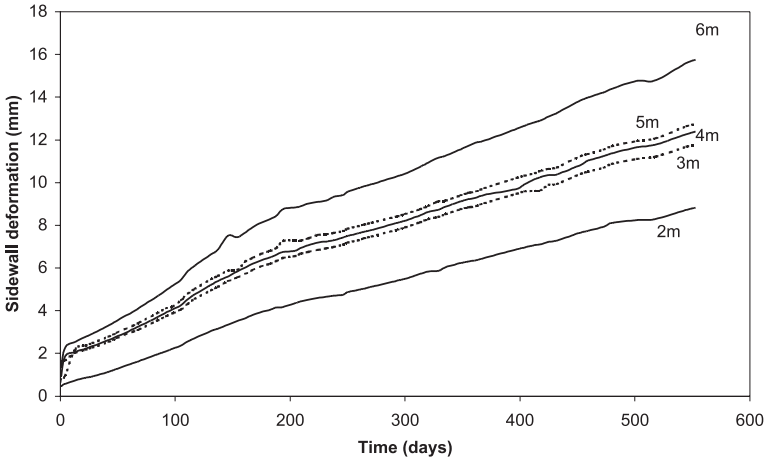

Fig. 11. Time-dependent deformation of the sidewall of a pump chamber measured with rod extensometers anchored at different depths. Note that the numerical results in Fig. 10 are absolute displacements, while the results in Fig. 11 are relative displacements between the skin of the excavation and the different anchor points inside the rock mass

3. Continuum Elasto-Viscoplastic Modelling

3.1 Introduction

As concluded in the previous section, a viscoelastic approach is not suitable to simulate the time-dependent behaviour of deep excavations in hard rock. From the work described in Malan (1998), it is evident that the time-dependent failure processes in the rock play a prominent role in the underground deformation behaviour. Any model used to simulate this time-dependent behaviour needs to include some representation of the delayed failure processes and the resulting time-dependent extension of the fracture zone. It appears as if the significant time-dependent effects are confined to the fracture envelope surrounding excavations. The far field behaviour has been shown to be adequately represented by elastic theory (Ryder and Officer, 1964). To simulate this behaviour, it is therefore necessary that the constitutive model is able to approximate the rheology of the fracture zone. To simulate the time-dependent fracture processes, the author developed a continuum elasto-viscoplastic model with a novel time-dependent weakening rule as described in the next section. This was implemented in the finite difference computer code FLAC.

To include failure processes in rheological models, slider elements (also called St. Venant elements) are typically added to the elastic and viscous elements of viscoelasticity. These slider elements have a specified failure strength and are immobilised below this strength. Commonly, a dashpot is placed in parallel with the slider to control the strain rate if the slider is loaded above its failure strength. This is the so-called Bingham unit.

Various combinations of elastic, viscous and St. Venant elements have been used by different researchers to simulate particular time-dependent problems. Gioda (1982) and Gioda and Cividini (1996) used a Kelvin unit in series with a

Bingham unit to represent primary and secondary closure in squeezing tunnels. Tertiary movements can be considered by providing suitable laws relating the values of the mechanical parameters (such as viscosity) to the irreversible part of the time-dependent strain. These rheological models are particularly suited for analysis carried out through the finite element method. This allows the interaction between squeezing rock and support to be simulated. Other examples of the use of these rheological models can be found in Akagi et al. (1984), Song (1993), Lee et al. (1995), Euverte et al. (1994) and Sagawa et al. (1995).

Since Perzyna (1966) proposed the general concept of elasto-viscoplasticity, a number of workers have applied this theory to geological materials. Elasto-viscoplasticity is essentially a modification of classical plasticity theory by the introduction of a time-rate rule in which the yield function and plastic potential function of classical plasticity are incorporated. In comparison with viscoelasticy, a viscoplastic material shows viscous behaviour in the plastic region only. Desai and Zhang (1987) used this theory together with a generalised yield function to characterise the viscoplastic behaviour of a sand and rock salt. Sepehr and Stimpson (1988) used Perzyna's theory as a basis to develop a time-dependent finite element model to understand the time-dependent closure of excavations and seismicity in the potash mines in Saskatchewan. For a rheological analysis of tunnel excavations, Swoboda et al. (1987) developed a coupled finite element/boundary element approach to analyse the interaction of the rock with the visco-elastic properties of the shotcrete. The rock was assumed to behave in an elasto-viscoplastic fashion.

Fakhimi (1992) and Fakhimi and Fairhurst (1994) proposed a visco-elastoplastic constitutive model to simulate the time-dependent behaviour of rock. The model consists of an elasto-plastic Mohr-Coulomb model in series with a linear viscous unit. This model was implemented in an explicit finite difference code. A typical solution cycle would be to do an elasto-plastic analysis during which real time is frozen. After an equilibrium point is reached, the linear viscous unit is used to determine additional creep strain components for a specified period of real time. Control is then passed back to the elasto-plastic analysis to obtain a new equilibrium and the process is repeated. Although this model appeared successful in imitating the behaviour of uniaxial and triaxial tests and the stand-up time of excavations, the time-dependent behaviour of the model is independent of the failure processes. The entire material (including the far field) also behaves in a viscous manner. This model is therefore not applicable to the conceptual model of deep excavations in hard rock where the time-dependency is a direct consequence of the failure processes and the solid rock behaves essentially elastically.

3.2 Model Formulation

A complete description of the model developed can be found in Malan (1999a). Figure 12 gives a representation of the developed model.

In this model, the intact rock behaves elastically, while a Mohr-Coulomb yield function determines the failure strength. Similar to classical viscoplasticity, the vis-

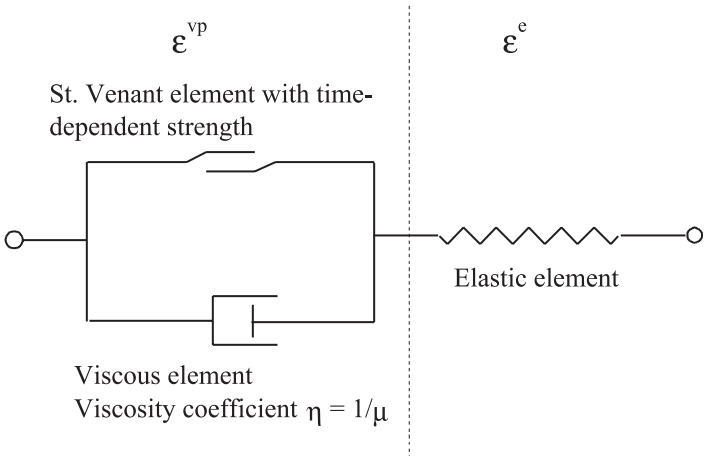

Fig. 12. Representation of the developed elasto-viscoplastic model

coplastic strain rate $\dot{\varepsilon}_i^{vp}$ after failure is given by

$$\dot{\varepsilon}_i^{vp} = \mu \langle f_s(t) \rangle \frac{\partial g_s}{\partial \sigma_i} \quad \text{for } i = 1, 2, 3, \tag{15}$$

where μ is the fluidity parameter, g_s is the plastic potential function, $f_S(t)$ is the yield function and σ_i is a principal stress. A constitutive description of time-dependent rock behaviour needs to include the effect of strength degradation with time and/or deformation. Observations of time-dependent fracturing ahead of tabular stopes and in some tunnels in the South African mines show that the rock becomes progressively more fractured with time, resulting in the gradual loss of cohesive strength in a particular volume of rock. This loss of strength was modelled by assuming that the rate of cohesion reduction $\dot{C}_c$ is proportional to the excess stress above the residual target surface.

$$\dot{C}_c = k_c \langle f_{res} \rangle, \tag{16}$$

where k_c is the cohesion decay factor and

$$f_{res} = \sigma_1 - \sigma_3 N_{\phi r} + 2C_r \sqrt{N_{\phi r}} \tag{17}$$

$$N_{\phi r} = \frac{1 + \sin \phi_r}{1 - \sin \phi_r} \tag{18}$$

is the residual target surface with C_r the residual cohesion and ϕ_r the residual friction angle. The principle embodied in Eq. (16) is based on the laboratory creep experiments described in Malan (1998) which indicated that if the rock specimens are loaded close to their failure strength, the creep rate and eventual creep failure occur faster than for a low stress. For a particular volume of rock under high stress, creep fractures will therefore form more rapidly, resulting in a faster loss of cohesion in the rock than for low stress.

Table 1. Model parameters used to simulate time-dependent fracture formation surrounding a tunnel

Parameter	Value
Vertical stress	70 MPa
Horizontal stress	40 MPa
Bulk modulus	27.7 GPa
Shear modulus	20.8 GPa
Density of the rock	2700 kg/m^3
Cohesion of intact rock	22 MPa
Friction angle (peak and residual)	30°
Residual cohesion	15 MPa
Cohesion decay	0.001 day^{-1}
Dilation angle	25°
Fluidity coefficient	1×10^{-11} Pa^{-1}.day^{-1}

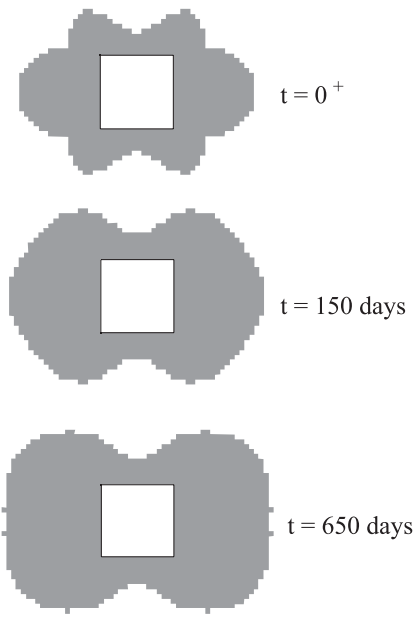

Fig. 13. Simulated time-dependent fracture zone formation surrounding a tunnel in elasto-viscoplastic rock subjected to constant field stresses. Note that this failure pattern is simply a plot of the failed zones in FLAC. This pattern looks different if contours of plastic strain are plotted

3.3 Simulation of Time-dependent Fracture Zone Behaviour

To illustrate the behaviour of the model described above, the time-dependent fracture zone formation surrounding a 4 m square tunnel subjected to constant field stresses was simulated. The model parameters are given in Table 1. Note that these parameters were arbitrarily chosen to illustrate the model behaviour.

The extent of the fracture zone at different times is illustrated in Fig. 13. Soon after development of the tunnel, the failed zone covers those areas where the

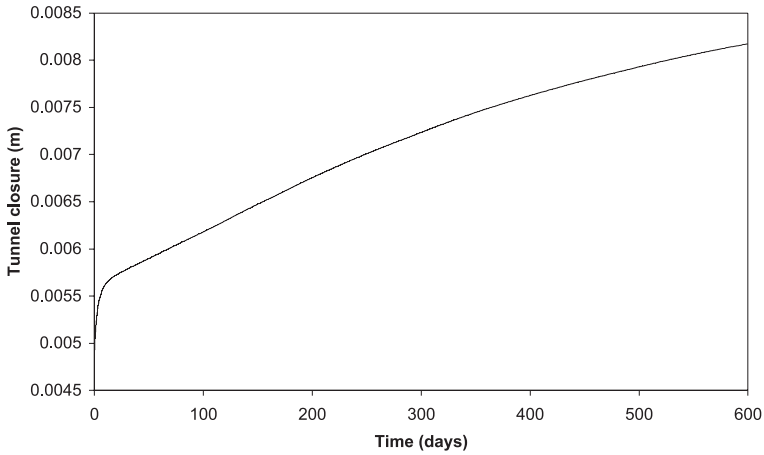

Fig. 14. Simulated tunnel closure (sidewall–sidewall) as a function of time caused by the time-dependent fracture zone formation described above

stresses exceeded the failure strength of the intact rock ($f_s(t) \leq 0$). Time-dependent processes lead to a gradual loss of residual strength in the fractured rock, transferring stress to the intact rock. This then also becomes fractured resulting in a time-dependent increase in the extent of the fracture zone as illustrated in Fig. 13. The resulting horizontal closure of the tunnel is illustrated in Fig. 14. The initial behaviour, soon after development, is dominated by the viscous response (Eq. 15) of the rock to changing stress conditions, which in this case are the induced stresses caused by the tunnel development. In the longer term, the behaviour is governed by the processes leading to a reduction in rock strength (Eq. 16). This leads to the steady-state closure regime visible in Fig. 14 between 50 and 300 days. If the field stresses remain constant, the closure will not continue indefinitely as an eventual equilibrium position is attained (unless very weak properties are used). This approach to the equilibrium position is visible in Fig. 14 as the gradual reduction in closure rate at the end of the data set. If the field stresses however continually increase over a period of time, the steady-state closure will also continue over this period.

This model proved to be more successful in modeling time-dependent closure in mining stopes as illustrated in Malan (1998).

4. Discontinuum Elasto-Viscoelastic Modelling

4.1 Need for a Discontinuum Model

When a tunnel is driven into soft squeezing rock (such as soft clays or mudstone), the ground advances slowly into the opening without visible fracturing or loss of continuity (Gioda and Cividini, 1996). Squeezing can, however, also involve different mechanisms of discontinuous failure of the surrounding rock. Possible mechanisms are complete shear failure in the rock if the existing discontinuities

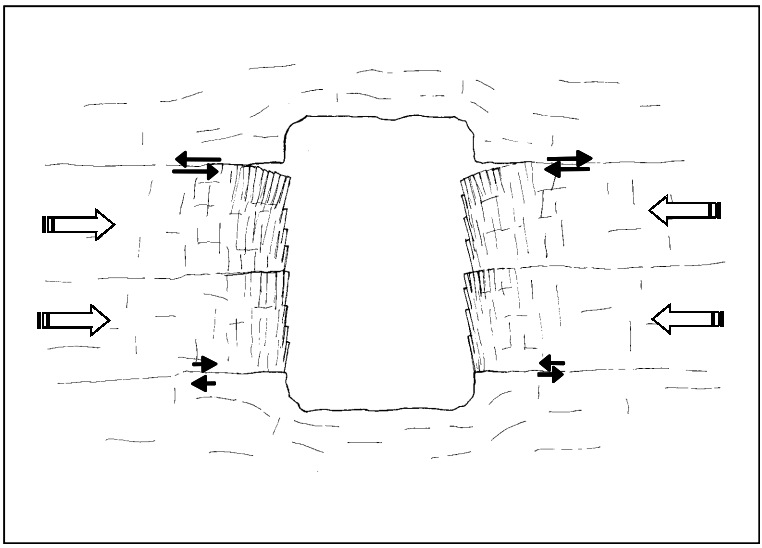

Fig. 15. Mechanism of squeezing tunnel deformation observed at Hartebeestfontein Mine (after Bosman et al., 2000)

are widely spaced, buckling failure in thinly bedded sedimentary rocks and sliding failure along bedding planes (Aydan et al., 1996).

As described in Section 1.1, squeezing conditions can be found in the deep access tunnels of Hartebeestfontein Gold Mine in South Africa. Figure 15 illustrates the mechanism of deformation observed in a tunnel located at No. 6 shaft Hartebeestfontein Mine at a depth of 2367 m. The host rock in this area comprises bedded quartzites with a uniaxial compressive strength ranging from 160 to 180 MPa for intact laboratory specimens. The tunnel is intersected by prominent bedding planes containing infilling with thickness up to 10 cm in some places. Significant shear displacement is observed on these bedding planes. The accompanying fracture processes and large deformations lead to the eventual destruction of the tunnel support as illustrated in Fig. 1. In these cases, a continuum elasto-viscoplastic formulation cannot be used to simulate the deformation and a different modelling approach is required.

4.2 Discontinuum Model Formulation

It is generally accepted that the time-dependent behaviour of excavations in hard rock is governed mainly by the rheological properties of discontinuities surrounding the excavation. This is in agreement with other workers (Tan and Kang, 1980; Schwartz and Kolluru, 1984). Barla (2000) noted that in conditions where discontinuities dominate the squeezing behaviour, discontinuum modelling is the most appropriate model to simulate the behaviour of the rock. Realistic modelling of the time-dependent behaviour of hard rock therefore needs to simulate the rheological behaviour of discontinuities and the interaction between these disconti-

nuities. Samtani et al. (1996) developed a viscoplastic interface model for use in finite element programs. Interface elements in finite element programs can however cause numerical problems through ill conditioning of the stiffness matrix and high stress gradients in the interface elements. (Day and Potts, 1994). Further difficulties are experienced in generating multiple discontinuities in finite element meshes. These problems are not encountered in boundary element programs. Napier and Peirce (1995) developed a boundary element method for solving multiple interacting crack problems in which several thousand elements can be treated. This formulation was used as modeling tool by the author to simulate the time-dependent behaviour of excavations in hard rock. To simulate the time-dependent behaviour of the discontinuities, a viscoplastic displacement discontinuity interface model was developed. In this model, it is postulated that the intact rock material behaves elastically and all inelastic behaviour, including viscoplastic effects is controlled by the presence of multiple interacting discontinuities. Shear slip on these discontinuities happens in a time-dependent fashion. This allows for the progressive redistribution of stress near the edges of mine openings. The detailed formulation of this model can be found in Napier and Malan (1997).

In summary, the model can be described as follows. Suppose that the local components of the displacement discontinuity vector are denoted by D_S for the shear and D_N for the normal component. Based on Perzyna's (1966) theory of plasticity, the rates of change in normal and shear discontinuity can then be given by

$$\begin{Bmatrix} \dfrac{\dot{D}_s}{d} \\ \dfrac{\dot{D}_n}{d} \end{Bmatrix} = \mu \langle F \rangle \begin{Bmatrix} \dfrac{\partial Q}{\partial \tau} \\ \dfrac{\partial Q}{\partial \sigma_n} \end{Bmatrix} \tag{19}$$

where F is the yield criterion, Q the plastic potential function, τ the shear stress acting on the discontinuity and σ_n the normal stress. It is postulated that the viscoplastic effects are limited to a finite discontinuity thickness d. This thickness not only includes gouge width and asperity heights but also the thin layer of rock adjacent to the discontinuity wall controlling the strength and deformation properties (Barton and Choubey, 1977). The intact rock between discontinuities behaves elastically. The fluidity μ is a material constant with units $\mathrm{Pa}^{-1}\mathrm{s}^{-1}$. For ease of model calibration the parameters μ and d will be grouped as $\kappa = \mu d$ with κ a surface fluidity parameter with units of $\mathrm{Pa}^{-1}\mathrm{s}^{-1}\mathrm{m}$. The Mohr-Coulomb model is adopted as yield criterion giving the following shear yield function.

$$F = |\tau| - S_C + \sigma_n \tan \phi_C, \tag{20}$$

where S_C and ϕ_C are the current values of cohesion and friction angle respectively. For an unmobilised discontinuity, $S_C = S_P$ and $\phi_C = \phi_P$ where S_P and ϕ_P are the peak values of cohesion and friction angle respectively. A negative stress convention is used for compressive stresses. Shear failure takes place for $F > 0$. Below the yield surface the discontinuity is immobilised. The function $\langle F \rangle$ in Eq. (19) implies that

$$\begin{aligned} \langle F \rangle &= F \quad \text{for } F \geq 0, \\ \langle F \rangle &= 0 \quad \text{for } F < 0. \end{aligned} \tag{21}$$

Roberts and Einstein (1978) showed that a non-associated flow rule should be adopted for rock joints. The plastic potential function is given by

$$Q = |\tau| + \sigma_n \tan \psi, \tag{22}$$

where ψ is the dilation angle. Inserting Eq. (22) in (19) and writing in incremental format gives

$$\begin{aligned} \Delta D_s &= \kappa \ell \langle F \rangle \Delta t \\ \Delta D_n &= |\Delta D_s| \tan \psi, \end{aligned} \tag{23}$$

where Δt is the time increment. The variable ℓ is introduced as a slip direction indicator where

$$\begin{aligned} \ell &= +1 \quad \text{for } \tau < 0, \\ \ell &= -1 \quad \text{for } \tau > 0. \end{aligned} \tag{24}$$

Napier and Malan (1997) and Malan (1998) used this model to simulate the time-dependent failure processes around tabular excavations. A good correlation between modelled and simulated stope closures were obtained in these studies. When setting up a particular model, the problem region of interest is covered by a specified mesh of potential crack surfaces. A random Delaunay mesh is used in this study with an example shown in Fig. 16. At the end of each timestep, the stress distribution in the model is calculated. The program then searches through the potential crack surfaces and activates those that will fail according to the specified Mohr-Coulomb failure criterion. The activated discontinuities then relax according to Eq. (19). The resulting stress distribution will lead to the activation of further crack surfaces as the program steps through time. This continues until an equilibrium condition is attained (depending on the chosen model parameters).

4.3 Numerical Simulation of Time-dependent Tunnel Deformation

The discontinuum model described above was used to simulate the mechanism of tunnel deformation at Hartebeestfontein Mine illustrated in Fig. 15. A square tunnel with dimensions of 3.4 m was simulated. Two parallel bedding planes with a dip angle of 9°, intersecting the sidewalls of the tunnel, were included. The geometry used is shown in Fig. 16. The other parameters used in the simulation are given in Table 2. It should be noted that the friction angles and cohesion are downgraded to simulate in situ conditions. Unfortunately no time-dependent tunnel deformation measurements are available for this particular site and therefore arbitrary values for the surface fluidity were used in this preliminary modelling attempt.

An important consequence of the imposed time-dependent displacement law imposed by Eq. (19) is that the fracture zone surrounding the excavation does not

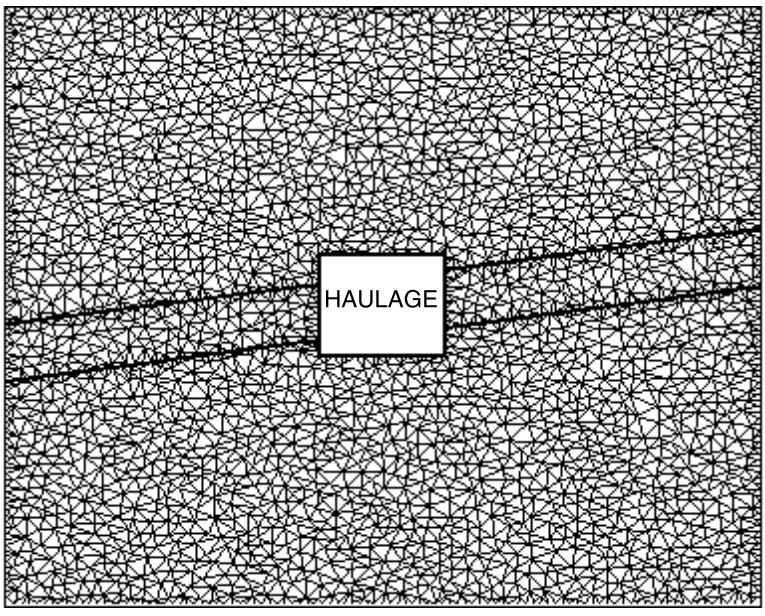

Fig. 16. Random mesh of potential fracture surfaces surrounding a tunnel. The thick lines represent the bedding planes. It should be emphasised that these elements are initially intact and only those that fail according to the failure criterion are included in the solution process. Also keep in mind that this is a boundary element formulation with infinite elastic boundaries. Although the potential fracture surfaces are only defined up to a certain distance from the tunnel, this should not be confused with a finite element or finite difference mesh

Table 2. Modelling parameters used

Parameter	Value
Young's modulus	70 GPa
Poisson's ratio	0.2
Vertical stress	110 MPa
Horizontal stress	71 MPa
Properties of intact rock:	
Intact friction angle	30°
Intact cohesion	20 MPa
Mobilized friction	30°
Mobilized cohesion	10 MPa
Surface fluidity	4×10^{-7} m.Pa^{-1}.day^{-1}
Properties of bedding planes:	
Friction angle	5°
Cohesion	0 MPa
Surface fluidity	4×10^{-7} m.Pa^{-1}.day^{-1}

form instantaneously but develops as a function of time. The discontinuities closer to the excavation fail first. They slip in a time-dependent fashion and gradually transfers the stress away from the tunnel where new fractures form. This is illustrated in Fig. 17. As a result of this behaviour, the sidewall closure also behaves in a time-dependent fashion. This is illustrated in Fig. 18. The bedding planes were

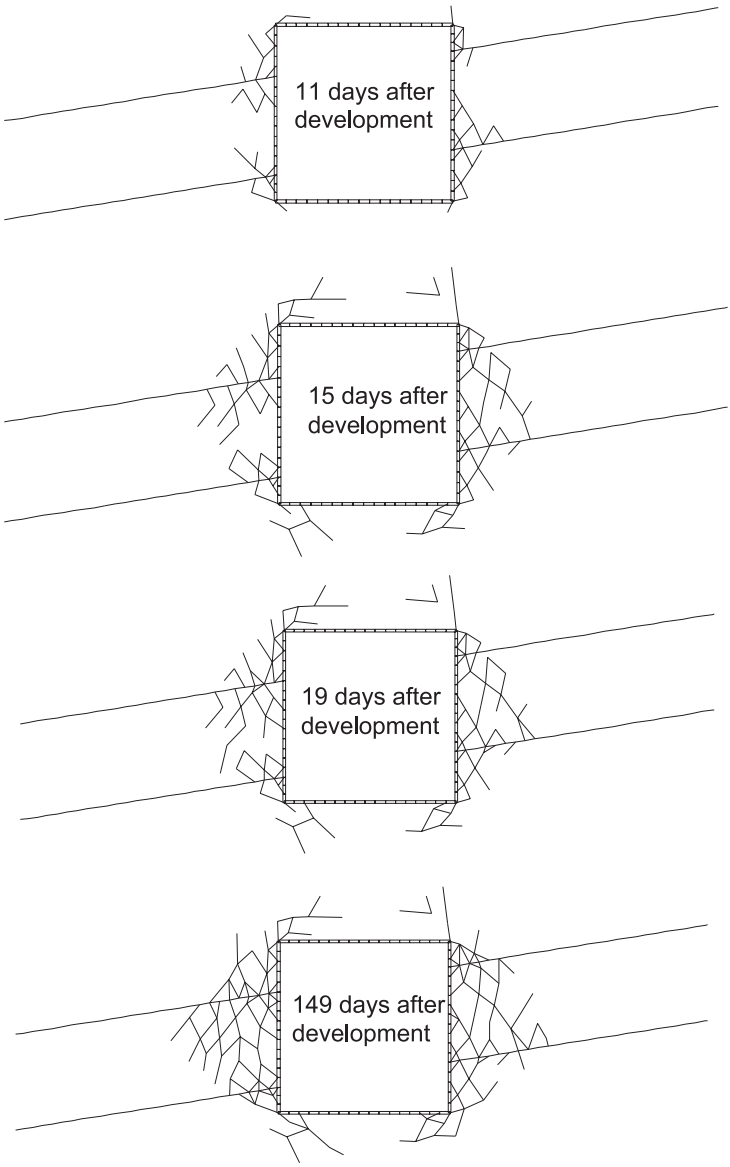

Fig. 17. Time-dependent evolution of the fracture zone after development of the tunnel

only mobilized from the tunnel sidewalls up to approximately 3.6 m. Of interest is that the slip on the bedding planes is low in spite of a low friction angle of 5°. This is illustrated in Fig. 19.

Apart from the tunnel simulations, the model was used successfully to simulate the time-dependent closure behaviour of tabular excavations as described in Malan (1998). Further work is currently conducted to verify that Eq. (19) is in fact

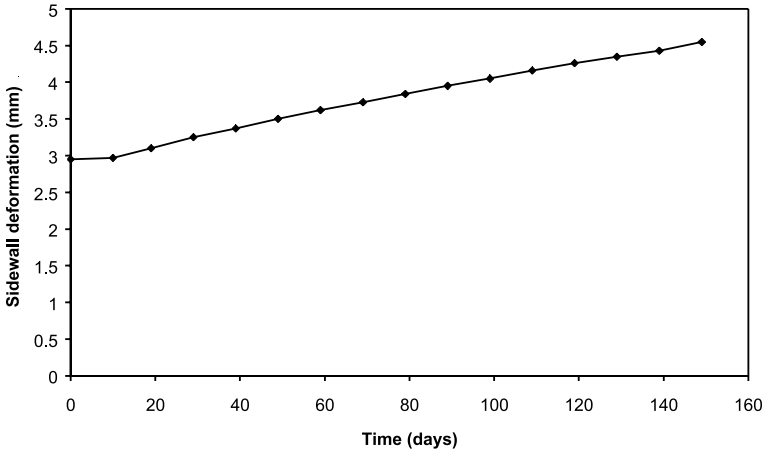

Fig. 18. Time-dependent deformation of the left sidewall

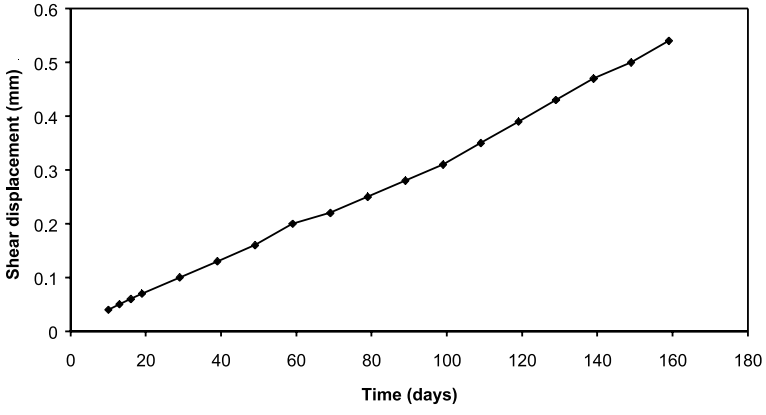

Fig. 19. Shear slip of one of the upper right bedding plane as a function of time. This is the deformation on the bedding plane at a distance of 0.8 m from the tunnel sidewall

the most appropriate constitutive law in this particular case and for hard rock in general.

5. Conclusions

Data collected from the tunnels and stopes of the deep South African mines illustrate significant time-dependent behaviour. Apart from application in mining, a better understanding of the time-dependent behaviour of crystalline rock is required to analyse the long term stability of nuclear waste repositories and to design better support for deep civil engineering tunnels in these rock types. To simulate the time-dependent behaviour of deep excavations in hard rock, the author investigated the following analytical and numerical approaches.

Viscoelasticy: To illustrate the subtle problems associated with using this theory, an analytical viscoelastic solution for the time-dependent closure of a tabular excavation mined in incremental steps is described in this study. Although this model gives a good fit with measured stope closure at a particular point in the stope, the calibrated solution does not necessarily give the correct results for other distances from the stope face. This is a result of the inability of viscoelastic theory to simulate the fracture zone around these excavations. This has important implications when using viscoelastic theory to simulate the time-dependent behaviour of tunnels surrounded by a zone of fractured material. Although a good fit can be obtained with a viscoelastic model and deformation measured on the skin of the excavation, it cannot be used to estimate the relative movement between the skin of the excavation and some point inside the rock mass.

Continuum elasto-viscoplasticy: A model based on classical viscoplasticity was developed and implemented in a finite difference code to simulate the formation of the fracture zone and the time-dependent behaviour of this zone around excavations. A novel time-dependent weakening rule was used to simulate the loss of cohesion in the near-field rock mass due to delayed fracture formation. This model proved successful in simulating the time-dependent stress transfer processes ahead of tabular excavations and the resulting time-dependent closure behaviour of mining stopes. It was also used to simulate the squeezing behaviour of some tunnels in these deep mines. The drawback of this continuum approach is its inability to simulate behaviour that is dominated by the creep of major discontinuities such as bedding planes.

Discontinuum viscoplasticity: A discontinuum viscoplastic approach was developed and implemented in a displacement discontinuity boundary element code. This allows explicit crack growth and development of these fractures in a time-dependent fashion. This approach was successful in simulating the time-dependent behaviour of the fracture zone around tabular excavations and the resulting time-dependent closure behaviour. The advantage of this model over the continuum approach is the ability to easily include bedding planes and the associated creep of these structures.

Acknowledgements

This work forms part of the rockmass behaviour research programme of Rock Engineering, CSIR Division of Mining Technology. The financial assistance and support received from the Safety in Mines Research Advisory Committee (SIMRAC) is acknowledged.

References

Akagi, T., Ichikawa, Y., Kuroda, H., Kawamoto, T. (1984): A non-linear rheological analysis of deeply located tunnels. Int. J. Numer. Anal. Meth. Geomech. 8, 457–471.

Aydan, Ö., Akagi, T., Kawamoto, T. (1996): The squeezing potential of rock around tunnels: Theory and prediction with examples taken from Japan. Rock Mech. Rock Engng. 29, 125–143.

Barla, G. (1995): Squeezing rocks in tunnels. ISRM News J. 2, 44–49.

Barla, G. (2000): Analysis and design methods of tunnels in squeezing rock conditions. Ital. Geotech J. 1, 22–29.

Barton, N., Choubey, V. (1977): The shear strength of rock joints in theory and practice. Rock Mech. 10, 1–54.

Blacic, J. D. (1981): Importance of creep failure of hard rock in the near field of a nuclear waste repository. In: Proc. Workshop on Nearfield Phenomenon in Geologic Repositories for Radioactive Waste, Seattle, 121–132.

Bosman, J. D., Malan, D. F., Drescher, K. (2000): Time-dependent tunnel deformation at Hartebeestfontein Mine. In: Stacey, T. R., Stimpson, R. G., Stimpson, J. L. (eds.) Proc. AITES – ITA 2000 – World Tunnel Congress, Tunnels under Pressure, Durban, 55–62.

Brox, D. R., Hagedorn, H. (1996): Prediction of in situ stresses based on observations and back analyses: Piora-Mulde exploratory tunnel, Gotthard Base Tunnel Project. In: Barla, G. (ed) Eurock '96, Prediction and performance in rock mechanics and rock engineering. Balkema, Rotterdam, 1047–1052.

Day, R. A., Potts, D. M. (1994): Zero thickness interface elements – numerical stability and application. Int. J. Numer. Anal. Meth. Geomech. 18, 689–708.

Desai, C. S., Zhang, D. (1987): Viscoplastic model for geologic materials with generalised flow rule. Int. J. Numer. Anal. Meth. Geomech. 11, 603–620.

Euverte, C., Allemandou, X., Dusseault, M. B. (1994): Simulation of openings in visco-elastoplastic media using a discrete element method. In: Siriwardane, H.-J. (ed.), Computer methods and advances in geomechanics. Balkema, Rotterdam, 809–814.

Fakhimi, A. A. (1992): The influence of time-dependent deformation of rock on the stability of underground excavations. PhD Thesis, University of Minnesota.

Fakhimi, A. A., Fairhurst, C. (1994): A model for the time-dependent behavior of rock. Int. J. Rock Mech. Min. Sci. 31, 117–126.

Flügge, W. (1975): Viscoelasticity, 2nd edn. Springer, Wien New York.

Gioda, G. (1982): On the non-linear "squeezing" effects around circular tunnels. Int. J. Numer. Anal. Meth. Geomech. 6, 21–46.

Gioda, G., Cividini, A. (1996): Numerical methods for the analysis of tunnel performance in squeezing rocks. Rock Mech. Rock Engng. 29, 171–193.

Italian Geotechnical Journal (2000): Special issue on squeezing rock conditions in tunneling. – March 2000.

Itasca (1993): FLAC – Fast Lagrangian Analysis of Continua: User's Manual.

Jaeger, J. C., Cook, N. G. W. (1979): Fundamentals of rock mechanics, 3rd edn. Chapman and Hall, London, 320.

Kwon, S. (2000): Suggestions for data analysis of in-situ deformation measurements from salt and potash mines. In: Girard, J., Liedman, M., Breeds, C., Doe, T. (eds.) Pacific Rocks 2000, Proc. 4th North American Rock Mech. Symp., Seattle, 1243–1248.

Kwon, S., Park, B. Y., Kang, C. H. (2000): Structural stability analysis for a high-level underground nuclear waste repository in granite. In: Girard, J., Liedman, M., Breeds, C., Doe, T. (eds.) Pacific Rocks 2000, Proc. 4th North American Rock Mech. Symp., Seattle, 1279–1285.

Lama, R. D., Vutukuri, V. S. (1978): Handbook on mechanical properties of rocks – Testing techniques and results – Vol. III. Trans Tech Publ. Clausthal, 209–320.

Lee, C., Lee, Y., Cho, T. (1995): Numerical simulation for the underground excavation-support sequence in the visco-plastic jointed rock mass. In: Fujii, T. (ed.) Proc. 8th Int. Cong. Rock Mech., ISRM. Balkema, Rotterdam, 619–621.

Malan, D. F. (1998): An investigation into the identification and modelling of time-dependent behaviour of deep level excavations in hard rock. PhD Thesis, University of the Witwatersrand, Johannesburg, South Africa.

Malan, D. F. (1999a): Time-dependent behaviour of deep level tabular excavations in hard rock. Rock Mech. Rock Engng. 32, 123–155.

Malan, D. F. (1999b): Implementation of a viscoplastic model in FLAC to investigate rate of mining problems. In: Detournay, C., Hart, R. (eds.) FLAC and Numerical Modelling in Geomechanics, Proc Int. FLAC Symp. on Num. Modelling in Geomech., Minnesota. Balkema, Rotterdam, 497–504.

Malan, D. F., Basson, F. R. P. (1998): Ultra-Deep Mining: The increased potential for squeezing conditions. J. S. Afr. Inst. Min. Metall. 98, 353–363.

Malan, D. F., Bosman, J. D. (1997): A viscoplastic approach to the modelling of time-dependent rock behaviour at Hartebeestfontein Gold Mine. In: Gürtunca, R. G., Hagan, T. O. (eds.) SARES97, Johannesburg, 117–130.

Malan, D. F., Drescher, K. (2000): Modeling the post-failure relaxation behaviour of hard rock. In: Girard, J., Liebman, M., Breeds, C., Doe, T. (eds.) Pacific rocks 2000, Proc. 4th North American Rock Mech. Symp., Seattle. 909–917.

Muirwood, A. M. (1972): Tunnels for roads and motorways. Quart. J. Eng. Geol. 5, 119–120.

Nakano, R. (1979): Geotechnical properties of mudstone and neogene tertiary in Japan. In: Proc. Int. Symp. Soil Mechanics, Oaxaca. 75–92.

Napier, J. A. L., Malan, D. F. (1997): A viscoplastic discontinuum model of time-dependent fracture and seismicity effects in brittle rock. Int. J. Rock Mech. Min. Sci. Geomech. Abstr. 34, 1075–1089.

Napier, J. A. L., Peirce, A. P. (1995): Simulation of extensive fracture formation and interaction in brittle materials. In: Rossmanith, H. P. (ed.) Mechanics of jointed and faulted rock, MJFR2. Balkema, Rotterdam, 63–74.

Pan, Y. W., Dong, J. J. (1991): Time-dependent tunnel convergence – I. Formulation of the model. Int. J. Rock Mech. Min. Sci. 28, 469–475.

Perzyna, P. (1966): Fundamental problems in viscoplasticity. Adv. Appl. Mech. 9, 243–377.

Pusch, R. (1993): Mechanisms and consequences of creep in crystalline rock. In: Hudson, J. A. (ed.) Comprehensive rock engineering, vol. 1. Pergamon Press, Oxford, 227–241.

Roberts, W. J., Einstein, H. A. (1978): Comprehensive model of rock discontinuities. J. A.S.C.E. 104, 553–569.

Robertson, E. C. (1964): Viscoelasticity of Rocks. In: Judd, W. R. (ed.) State of stress in the earth's crust. Proc. Int. Conf., Santa Monica, California, 181–233.

Ryder, J. A., Officer, N. C. (1964): An elastic analysis of strata movement observed in the vicinity of inclined excavations. J. S. Afr. Inst. Min. Metall. 64, 219.

Sagawa, Y., Yamatomi, J., Mogi, G. (1995): A rheology model for non-linear and time-dependent behaviour of rocks. In: Fujii, T. (ed.) Proc. 8th Int. Cong. Rock Mech. ISRM. Balkema, Rotterdam, 311–314.

Salamon, M. D. G. (1968): Two-dimensional treatment of problems arising from mining tabular deposits in isotropic or transversely isotropic ground. Int. J. Rock Mech. Min. Sci. 5, 159–185.

Salamon, M. D. G. (1974): Rock mechanics of underground excavations. In: Proc. 3rd Congress Int. Society for Rock Mechanics 951–1099.

Samtani, N. C., Desai, C. S., Vulliet, L. (1996): An interface model to describe viscoplastic behaviour. Int. J. Numer. Anal. Meth. Geomech. 20, 231–252.

Schwartz, C. W., Kolluru, S. (1984): The influence of stress level on the creep of unfilled rock joints. In: Proc. 25th Symp. Rock Mech. 333–340.

Sepehr, K., Stimpson, B. (1988): Potash mining and seismicity: A time-dependent finite element model. Int. J. Rock Mech. Min. Sci. Geomech. Abstr. 25, 383–392.

Song, D. (1993): Non-linear viscoplastic creep of rock surrounding an underground excavation. Int. J. Rock Mech. Min. Sci. Geomech. Abstr. 30, 653–658.

Swoboda, G., Mertz, W., Beer, G. (1987): Rheological analysis of tunnel excavations by means of coupled finite element (FEM)-boundary element (BEM) analysis. Int. J. Numer. Anal. Meth. Geomech. 11, 115–129.

Tan, T., Kang, W. (1980): Locked in stresses, creep and dilatancy of rocks, and constitutive equations. Rock Mech. 13, 5–22.

Appendix I. Deriving a Viscoelastic Convergence Solution for Tabular Excavations

Salamon (1968) calculated the elastic convergence (S_z) of a parallel-sided panel (see Fig. 5) in isotropic ground without contact between the hangingwall and footwall as

$$S_z(x) = \frac{-4(1-\nu^2)W_z}{E}\sqrt{\ell^2 - x^2}\left(1 + \frac{dx}{2}\right), \tag{I.1}$$

where

$$W_z = \frac{-\rho g H}{2}[(1+k) + (1-k)\cos 2\alpha], \tag{I.2}$$

and

$$d = \frac{\sin\alpha\cos\beta}{H}, \tag{I.3}$$

where 2ℓ is the span of the stope, ρ is the density of the rock, g is the gravitational acceleration, H is the depth below surface, k is the ratio of horizontal to vertical stress, α is the dip of the reef, β is the angle between x-axis and the dip, ν is Poisson's ratio and E is Young's modulus.

Any viscoelastic model can be described by a differential equation of the form (Flügge, 1975)

$$\sigma + p_1\dot{\sigma} + p_2\ddot{\sigma} + \cdots = q_0\varepsilon + q_1\dot{\varepsilon} + q_2\ddot{\varepsilon} + \cdots \tag{I.4}$$

or

$$P\sigma = Q\varepsilon, \tag{I.5}$$

where

$$P = \sum_{k=0}^{m} p_k \frac{d^k}{dt^k} \quad Q = \sum_{k=0}^{n} q_k \frac{d^k}{dt^k}, \tag{I.6}$$

with σ the stress tensor, ε the strain tensor and $p_0 = 1$. Subjecting Eq. (I.5) to the Laplace transformation gives

$$\tilde{P}(s)\tilde{\sigma}(s) = \tilde{Q}(s)\tilde{\varepsilon}(s), \tag{I.7}$$

where

$$\tilde{P}(s) = \sum_{k=0}^{m} p_k s^k \quad \tilde{Q}(s) = \sum_{k=0}^{n} q_k s^k. \tag{I.8}$$

When doing an analysis of strain in a viscoelastic material, the stress and strain tensors can be divided in two representing dilatation and distortion (see Flügge, 1975). Eq. (I.5) then becomes

$$P'\sigma_m = Q'\varepsilon_m \tag{I.9}$$

$$P''\sigma_d = Q''\varepsilon_d, \tag{I.10}$$

with Eq. (I.9) representing dilatation (hydrostatic compression) and Eq. (I.10) distortion. In these equations, σ_m and ε_m are the dilational stress and strain and σ_d and ε_d the distortional stress and strain. In the limiting case of an elastic solid, Hooke's law for an isotropic medium may be written as (Jaeger and Cook, 1979)

$$\sigma_m = 3K\varepsilon_m \tag{I.11}$$

$$\sigma_d = 2G\varepsilon_d, \tag{I.12}$$

where K and G are the bulk and shear modulus respectively. In the Laplace domain, Eq. (I.9), (I.10), (I.11) and (I.12) become

$$\tilde{P}'(s)\tilde{\sigma}_m(s) = \tilde{Q}'(s)\tilde{\varepsilon}_m(s), \tag{I.13}$$

$$\tilde{P}''(s)\tilde{\sigma}_d(s) = \tilde{Q}''(s)\tilde{\varepsilon}_d(s), \tag{I.14}$$

$$\tilde{\sigma}_m(s) = 3K\tilde{\varepsilon}_m(s), \tag{I.15}$$

$$\tilde{\sigma}_d(s) = 2G\tilde{\varepsilon}_d(s). \tag{I.16}$$

Therefore for an elastic material when choosing $\tilde{P}'(s) = 1$ and $\tilde{P}''(s) = 1$, it follows that

$$\tilde{Q}'(s) = 3K \quad \tilde{Q}''(s) = 2G. \tag{I.17}$$

Dividing (I.13) by (I.15) and (I.14) by (I.16) gives

$$K = \frac{\tilde{Q}'(s)}{3\tilde{P}'(s)}, \tag{I.18}$$

$$G = \frac{\tilde{Q}''(s)}{2\tilde{P}''(s)}. \tag{I.19}$$

Writing Eq. (I.18) and (I.19) in terms of Young's Modulus (E) and Poisson's Ratio (v) gives

$$\tilde{E} = \frac{3\tilde{Q}''\tilde{Q}'}{2\tilde{P}''\tilde{Q}' + \tilde{Q}''\tilde{P}'}, \tag{I.20}$$

$$\tilde{v} = \frac{\tilde{P}''\tilde{Q}' - \tilde{Q}''\tilde{P}'}{2\tilde{P}''\tilde{Q}' + \tilde{Q}''\tilde{P}'}. \tag{I.21}$$

Subjecting Eq. (I.1) to the correspondence principle gives

$$\tilde{S}_z = \frac{-4(1-\tilde{v}^2)\tilde{W}_z}{\tilde{E}}\sqrt{\ell^2 - x^2}\left(1 + \frac{dx}{2}\right). \tag{I.22}$$

Assuming that W_z does not change with time gives

$$\tilde{W}_z(s) = \frac{W_z}{s}. \tag{I.23}$$

Substituting the Eq. (I.20), (I.21) and (I.23) in Eq. (I.22) and transforming back to the time domain gives

$$S_z(x,t) = -4W_z F(t)\sqrt{\ell^2 - x^2}\left(1 + \frac{dx}{2}\right), \tag{I.24}$$

where

$$F(t) = L^{-1}\left[\frac{\tilde{P}''^2\tilde{Q}' + 2\tilde{P}''\tilde{P}'\tilde{Q}''}{s\tilde{Q}''(2\tilde{P}''\tilde{Q}' + \tilde{P}'\tilde{Q}'')}\right]. \tag{I.25}$$

The symbol L^{-1} is used to signify the inverse Laplace transformation. To obtain the final solution, the inverse Laplace transformation in Eq. (I.25) must be determined for the appropriate viscoelastic model.

I.1 Viscoelastic Convergence Solution for a Burgers Model

The Burgers model can be constructed by combining a Maxwell and Kelvin model (Fig. 6). If it is assumed that the rock behaves as an elastic solid in dilatation and like a Burgers model in distortion, the following differential equation can be derived for the distortional part. Although the general equation of the Burgers model is known in the form of Eq. (I.4) (Flügge, 1975), the following analysis for the distortional component is necessary to determine the coefficients p_1, p_2, q_1 and q_2 in terms of the viscosity coefficients η_1 and η_2 and shear moduli G_1 and G_2. For the Maxwell component it can be shown that

$$\sigma_d + p_1'\dot{\sigma}_d = q_1'\dot{\varepsilon}_d', \tag{I.26}$$

where

$$p_1' = \frac{\eta_2}{2G_2} \quad q_1' = \eta_2. \tag{I.27}$$

For the Kelvin component it follows that

$$\sigma_d = q_0'' \varepsilon_d'' + q_1'' \dot{\varepsilon}_d'', \tag{I.28}$$

where

$$q_0'' = 2G_1, \quad q_1'' = \eta_1. \tag{I.29}$$

Taking the Laplace transformation of Eqs. (I.26) and (I.28) gives

$$(1 + p_1' s)\tilde{\sigma}_d = q_1' s \tilde{\varepsilon}_d' \tag{I.30}$$

$$\tilde{\sigma}_d = (q_0'' + q_1'' s)\tilde{\varepsilon}_d''. \tag{I.31}$$

Multiplying each equation with a suitable constant and adding gives

$$(1 + p_1' s)(q_0'' + q_1'' s)\tilde{\sigma}_d + q_1' s \tilde{\sigma}_d = q_1' s (q_0'' + q_1'' s)\tilde{\varepsilon}_d, \tag{I.32}$$

where

$$\tilde{\varepsilon}_d = \tilde{\varepsilon}_d' + \tilde{\varepsilon}_d''. \tag{I.33}$$

Taking the inverse Laplace transformation and inserting Eq. (I.27) and (I.29) gives

$$\sigma_d + p_1 \dot{\sigma}_d + p_2 \ddot{\sigma}_d = q_1 \dot{\varepsilon}_d + q_2 \ddot{\varepsilon}_d, \tag{I.34}$$

where

$$p_1 = \frac{q_1'' + p_1' q_0'' + q_1'}{q_0''} = \frac{\eta_1 G_2 + \eta_2 G_1 + \eta_2 G_2}{2G_1 G_2} \tag{I.35}$$

$$p_2 = \frac{p_1' q_1''}{q_0''} = \frac{\eta_1 \eta_2}{4G_1 G_2} \tag{I.36}$$

$$q_1 = q_1' = \eta_2 \tag{I.37}$$

$$q_2 = \frac{q_1' q_1''}{q_0''} = \frac{\eta_1 \eta_2}{2G_1}. \tag{I.38}$$

When subjecting Eq. (I.34) to the Laplace transformation gives

$$(1 + p_1 s + p_2 s^2)\tilde{\sigma}_d = (q_1 s + q_2 s^2)\tilde{\varepsilon}_d. \tag{I.39}$$

If the rock behaves elastically in dilatation and according to a Burgers model in distortion it therefore follows from Eq. (I.13), (I.14), (I.15) and (I.39) that

$$\tilde{P}' = 1 \quad \tilde{P}'' = 1 + p_1 s + p_2 s^2 \quad \tilde{Q}' = 3K \quad \tilde{Q}'' = q_1 s + q_2 s^2. \tag{I.40}$$

When Eq. (I.40) is substituted into (I.25)

$$F(t) = L^{-1}\left[\frac{3K(1 + p_1 s + p_2 s^2)^2 + 2(1 + p_1 s + p_2 s^2)(q_1 s + q_2 s^2)}{s(q_1 s + q_2 s^2)[6K(1 + p_1 s + p_2 s^2) + (q_1 s + q_2 s^2)]}\right]. \tag{I.41}$$

Finding the inverse Laplace transformation by partial fraction expansion gives (see Malan, 1998)

$$F(t) = g_1[1 + c_5 t + c_6 e^{-ft} + (c_7 \sinh bt + c_8 \cosh bt)e^{-ht/2}], \tag{I.42}$$

where the parameters $b, g_1, c_5, c_6, c_7, c_8, f$ and h is given by Eqs. (6) to (12). The complete convergence solution for the Burgers model is obtained by inserting Eq. (I.42) in (I.24).

I.2 Dealing with Incremental Face Advance

Equation (I.24) is applicable to situations where the total length of the tabular excavation is mined instantaneously. This is not the case in practice where the face is incrementally advanced. Assume that the first mining increment is created at time τ_1 giving a stope of half span L. Equation (I.24) will give the viscoelastic convergence for this step as $S_z(\ell = L, x, t - \tau_1)$. At time τ_2 the face is advanced on both sides of the stope by $\Delta\ell$ giving a half span of $(L + \Delta\ell)$. Using Eq. (I.24) with a half span of $(L + \Delta\ell)$ at time τ_2 results in the total span being created in one step, which is clearly wrong. At time $\tau_2 + \Delta t$ the total viscoelastic convergence is the sum of the viscoelastic convergence caused by a half span of L (excavated at time τ_1) plus an incremental viscoelastic convergence caused by the incremental length $\Delta\ell$, excavated at time τ_2. The incremental viscoelastic convergence is the difference between the viscoelastic convergence of a stope with half span $L + \Delta\ell$ created at time τ_2 and the viscoelastic convergence of a stope with half span L also created at time τ_2. Therefore at time $\tau_2 + \Delta t$ the viscoelastic convergence is given as

$$S_z = S_z(\ell = L, x, t - \tau_1) + S_z(\ell = L + \Delta\ell, x, t - \tau_2) - S_z(\ell = L, x, t - \tau_2). \tag{I.43}$$

Salamon (1974) used arguments of negative and positive superposition to give a general expression for an arbitrarily shaped excavation created in n increments as

$$u = \left\{ \sum_{i=1}^{n-1} [F_i(l_i, t - \tau_i)] - [F_i(l_i, t - \tau_{i+1})] \right\} + F_n[l_n, t - \tau_n] \tag{I.44}$$

which is valid for $\tau_n \leq t < \tau_{n+1}$ where u is the displacement component at some point in the rock, F_i is some function dependent on the shape of the excavation and l_i is a critical linear dimension of the excavation.

If the shape of the excavation stays constant ($F_1 = F_2 = F$) and $n = 2$, then Eq. (I.44) is reduced to Eq. (I.43) with $F = S_z$. Equation (2) is obtained by writing (I.44) in the notation used for the tabular excavations.

Author's address: Dr. F. Malan, CSIR Mining Technology, Johannesburg, South Africa, e-mail: FMALAN@csir.co.za